

# Titanium aluminides from cold-extruded elemental powders with Al-contents of 25–75 at % Al

G.-X. WANG, M. DAHMS

*Institut für Werkstofforschung, GKSS, Geesthacht, Germany*

G. LEITNER, S. SCHULTRICH

*Fraunhofer-Einrichtung für Keramische Technologien und Sinterwerkstoffe, IKTS, Dresden, Germany*

Titanium aluminide alloys were prepared from cold-extruded elemental Ti and Al powders with compositions ranging from 25 to 75 at % Al. The production route in this study includes four essential steps: mixing, precompaction, cold-extrusion and reaction treatment. During reaction treatment, the intermetallic phases  $Ti_3Al$ ,  $TiAl$  and  $TiAl_3$  are formed by interdiffusion of Ti and Al, and pore formation takes place because of the different diffusivities of Ti and Al. The processes of phase formation, as well as pore formation, were studied by means of calorimetric, dilatometric and metallographic methods. In order to obtain nearly fully dense specimens, the technique of hot isostatic pressing was applied. The sintering behaviour and microstructures of the prepared alloys are reported.

## 1. Introduction

Intermetallic phases have an intermediate position between the relatively soft and ductile superalloys and the hard and extremely brittle ceramics. The application of superalloys with a good combination of strength and toughness is limited to temperatures below 1100 °C, whereas modern engineering ceramics can be used at much higher temperatures [1]. Among the numerous intermetallic phases, titanium aluminides are considered as lightweight materials for applications to span the range between superalloys and ceramics, due to their low densities, high melting temperatures, relatively good high temperature mechanical properties and environmental resistance. Titanium aluminide alloys are mostly produced using ingot metallurgy. However, the poor workability of titanium aluminides suggests further studies on a production route starting with elemental powders [2, 3]. With this production route, near net-shaped components can be fabricated so that the poor workability of titanium aluminides can be avoided. Moreover, it is possible to prepare alloys with arbitrary compositions and different additives. These are major advantages of this processing over the ingot and prealloyed powder processing routes. The present paper reports on the production of titanium aluminide alloys with compositions ranging from 25 to 75 at % Al from cold-extruded elemental powders. Emphasis is placed on the phase formation, sintering behaviour and microstructures.

## 2. Experimental procedure

### 2.1. Production route

The process starts with elemental Ti and Al powders and includes the following steps: mixing, precompaction, cold extrusion, and reaction treatment. Cold extrusion is beneficial, as the porosity formed during reaction treatment is considerably less than the porosity of simply compacted powder mixture. The porosity is strongly influenced by the extrusion ratio,  $\phi$ , which is defined as the area ratio of specimen cross sections before ( $A_1$ ) and after extrusion ( $A_2$ ). For example, the

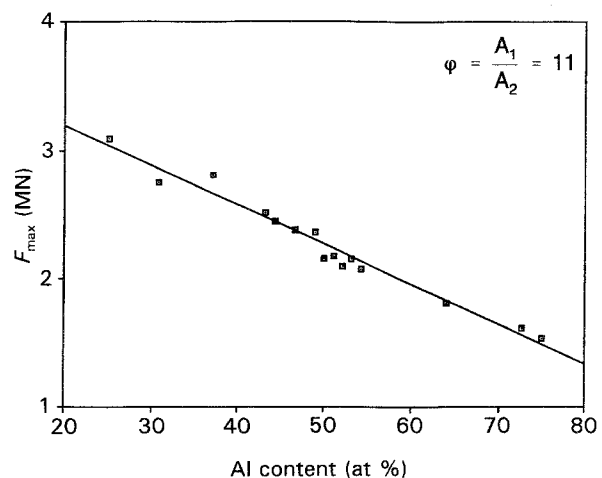


Figure 1 Maximum extrusion load as a function of powder composition.

porosity in the powder mixture Ti-48 at % Al after pressureless sintering at 1350 °C for 6 h is about 16%, and less than 2% for specimens extruded with extrusion ratios of 17 and 350, respectively [4]. The

extruded pieces can easily be machined into different shapes, as intermetallic phases are not present at this stage. Reaction treatment is carried out as the last step to obtain the desired intermetallics  $Ti_3Al$ ,  $TiAl$  and

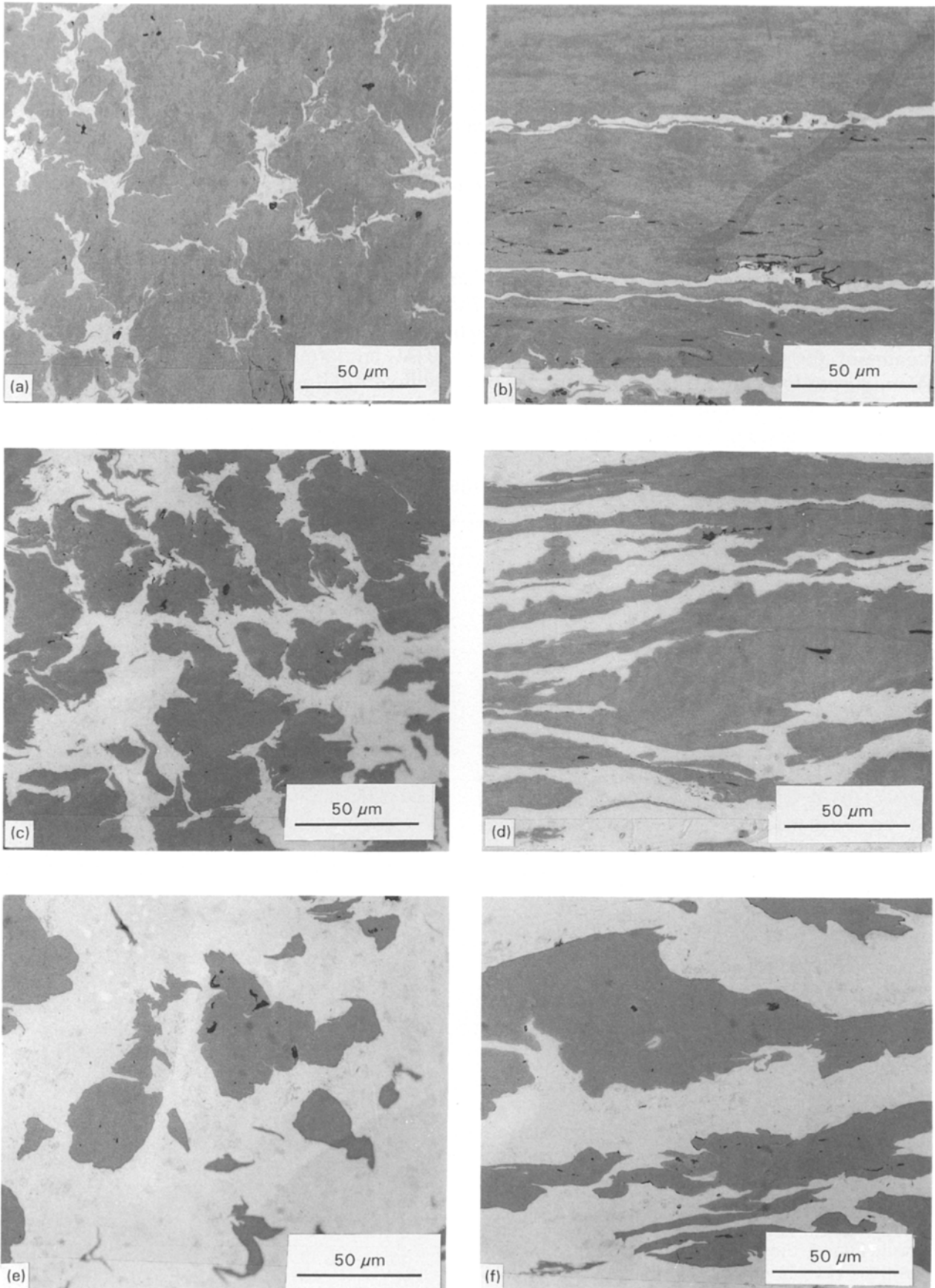


Figure 2 As-extruded microstructure of the three stoichiometric compositions: (a, b)Ti-25Al; (c, d) Ti-50Al; (e, f) Ti-75Al, in sections perpendicular (a, c, e) and parallel (b, d, f) to the extrusion direction.

TiAl<sub>3</sub>. If the reaction treatment is conducted without applying external pressure, pore formation takes place due to Kirkendall diffusion and capillarity. The Al atoms move into Ti-particles, whereas the Ti atoms remain almost immobile [5]. Such a one-sided diffusion (Kirkendall diffusion) leads to pore formation in the solid state. At temperatures above the Al melting point, Al melt flows away along particle or grain boundaries due to capillarity, also causing pore formation [4]. Therefore, applying the technique of hot isostatic pressing (HIP) is necessary in order to compress pores formed during reaction treatment. Encapsulation prior to HIP is normally needed due to open pores. However, this expensive stage could be excluded by applying a high enough extrusion ratio to yield a small porosity. Efforts have already been made to produce nearly pore-free material prepared by HIPing without encapsulation (extrusion ratio = 350) [6].

## 2.2. Powder consolidation

Elemental powders smaller than 150 μm in size were mixed in air using a tumbling mixer. The composition was varied in the range 25–75 at % Al. The powders were water-atomized aluminium and titanium sponge of 99.5% purity. A green compact was prepared at room temperature under 1000 kN load. Compacted billets were extruded at room temperature with an extrusion ratio of 11. During extrusion, the load quickly increases to a maximum and then slowly decreases. The maximum load increases with increasing Ti content, as shown in Fig. 1.

## 3. Results and discussion

### 3.1. Powder consolidation

Fig. 2 shows the as-extruded microstructures of three specimens with compositions of the stoichiometric Ti<sub>3</sub>Al, TiAl and TiAl<sub>3</sub> i.e. Ti–25Al, Ti–50Al and Ti–75Al (at %). Both Ti and Al, appearing as dark and white regions, respectively, are elongated in the extrusion direction. The size of Al regions, which decides the pore size as well as the porosity [4, 6], decreases with increasing Ti content.

### 3.2. Thermal analysis

Using a differential scanning calorimeter (DSC) and a high-temperature dilatometer, the thermal responses of the three specimens shown in Fig. 2 were studied. Both calorimetric and dilatometric investigations were carried out in a large temperature range to 1400 °C and at five different heating rates, β: 0.2, 1, 5, 20 and 50 K min<sup>-1</sup>.

The results of the DSC experiments are shown in Fig. 3. All DSC measurements were stopped at about 1000 °C, as no distinct thermal effects were observed at high temperatures. In Fig. 3, arbitrary units are used, because for each heating rate a specific measuring sensitivity is valid.

The DSC curves in Fig. 3 clearly show two exothermal effects. The first appears at temperatures below 660 °C (the Al melting point). The corresponding

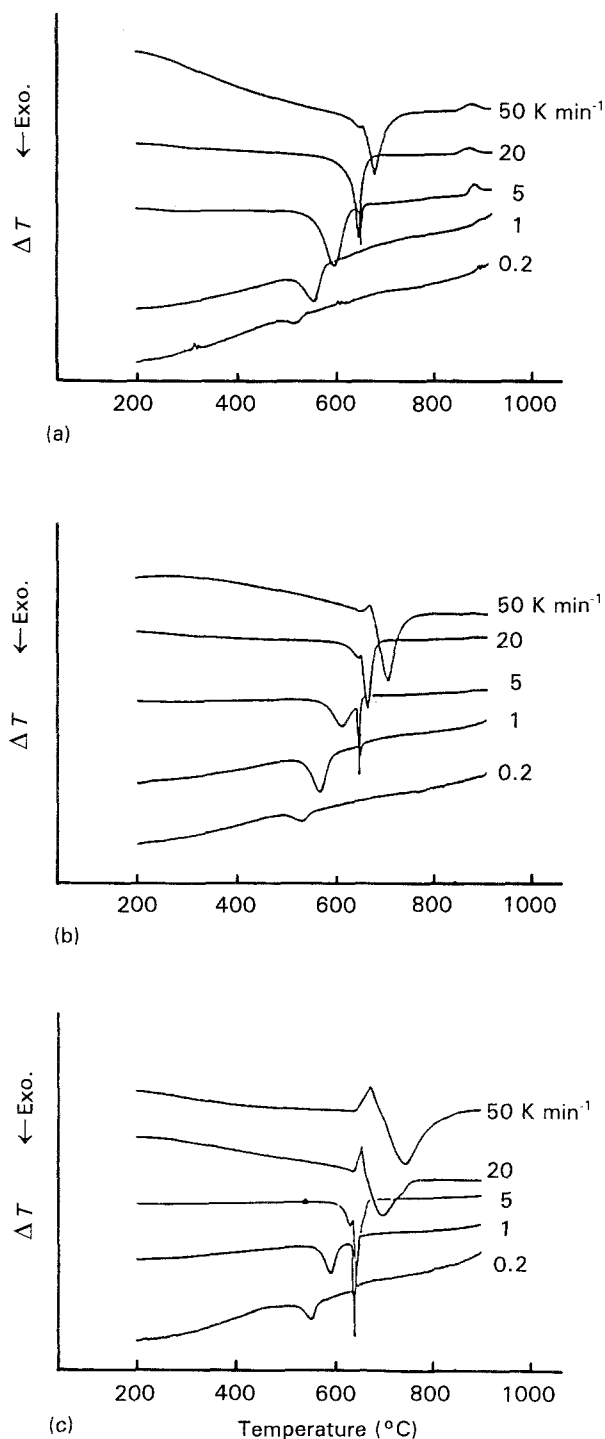


Figure 3 DSC curves of three stoichiometric compositions: (a) Ti–25Al; (b) Ti–50Al; (c) Ti–75Al.

maximum temperature,  $T_{max}$ , is a function of both heating rate and composition (Fig. 4). For the same composition, it rises with increasing heating rate. At a constant heating rate,  $T_{max}$  increases with increasing Al content. Assuming this effect is due to a single solid-state reaction, the shift of the exothermal maximum temperature,  $T_{max}$ , with heating rate β can be analysed according to Kissinger [7]. Fig. 5 shows the Kissinger plots for the three stoichiometric compositions. All three Kissinger plots exhibit the same slope, which gives an activation energy of  $200 \pm 20$  kJ mol<sup>-1</sup>. The same value was also determined for the cold-extruded elemental powder mixture Ti–49Al [8, 9]. This activation energy is in agreement with that for TiAl<sub>3</sub> layer

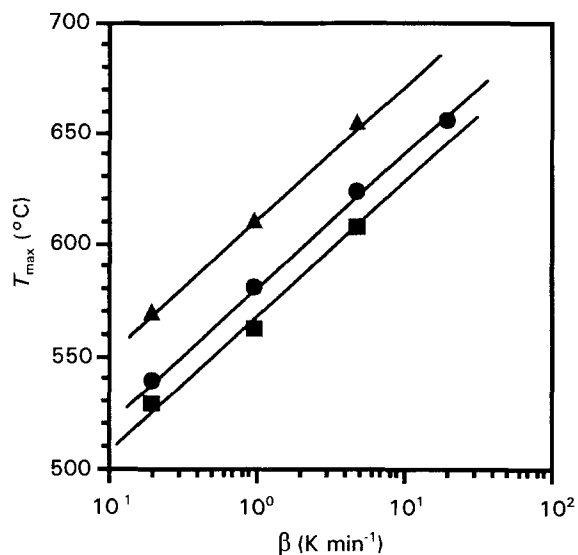


Figure 4 Maximum temperature as a function of both heating rate and composition. ■, Ti-25Al; ●, Ti-50Al; ▲, Ti-75Al.

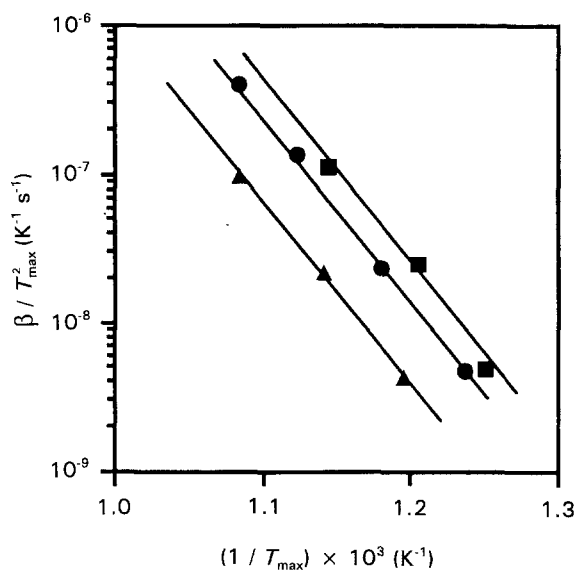


Figure 5 Kissinger plots of the three stoichiometric compositions. ■, Ti-25Al; ●, Ti-50Al; ▲, Ti-75Al.

growth by interdiffusion between Ti and Al, determined by van Loo & Rieck [5]. Therefore the first exothermal effect shown by the DSC curves is due to the solid reaction  $\text{Ti} + \text{Al} \rightarrow \text{TiAl}_3$ .

The second exothermal effect is dominantly present at higher heating rates and at higher Al contents (Fig. 3). The nearly constant starting temperature of the second effect close to the Al melting point is certainly due to a liquid–solid reaction. As local superheating due to formation of  $\text{TiAl}_3$  can lead to local Al melting, the measured starting temperature of the second effect is slightly below the Al melting point. Local melting leads to an instantaneous reaction between molten Al and solid Ti. Under action of capillary forces, the Al melt is quickly spread over new unreacted Ti surfaces, forming further intermetallic phase  $\text{TiAl}_3$ . This has been experimentally confirmed by Dahms *et al.* [9] with the help of optical and scanning electron microscopy as well as X-ray analysis

and diffractometry. The rate of this process is so high that it cannot be resolved by calorimetry, if the amount of Al melt is not very large, so neither an endothermal overall Al melting peak nor an extra exothermal reaction peak can be clearly observed in the case of Ti-25Al and Ti-50Al. Only in the case of Ti-75Al, endothermal Al melting peaks can be seen at high heating rates of 20 and 50  $\text{K min}^{-1}$  (Fig. 3c). At low heating rates, the time for solid–solid reaction is long and Al may have reacted completely below the Al melting point, especially in the case of low Al contents. This can be clearly seen by comparison of the DSC curves for the heating rate of 1  $\text{K min}^{-1}$  (Fig. 6). At

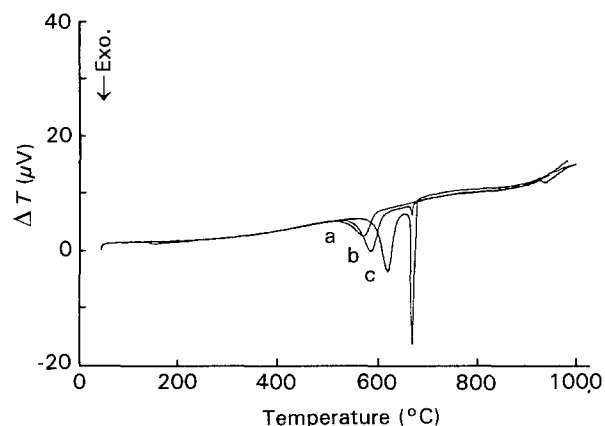


Figure 6 Comparison between DSC curves of the three stoichiometric compositions at a heating rate of 1  $\text{K min}^{-1}$ . (a) Ti-25Al; (b) Ti-50Al; (c) Ti-75Al.

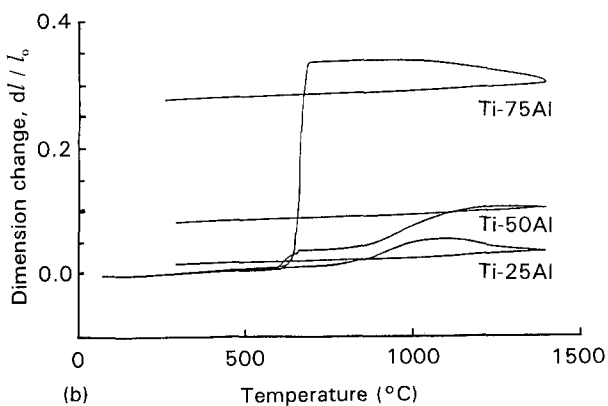
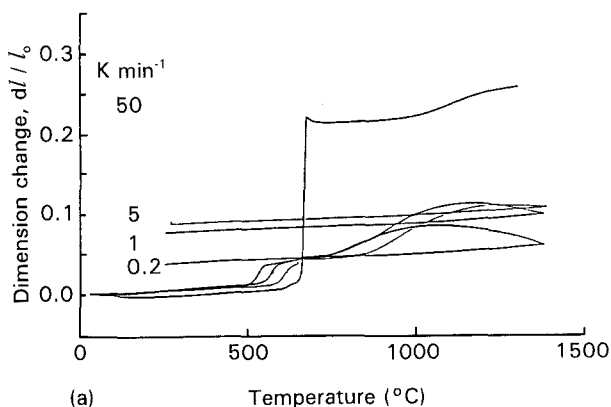


Figure 7 Dilatometric curves of (a) extruded Ti-50Al at different heating rates and (b) dilatometric curves of the three stoichiometric compositions at a heating rate of 5  $\text{K min}^{-1}$ .

this heating rate, the second effect completely disappears in Ti-25Al and is very small in Ti-50Al.

Further heating of specimens of Ti-25Al and Ti-50Al to higher temperatures leads to the formation

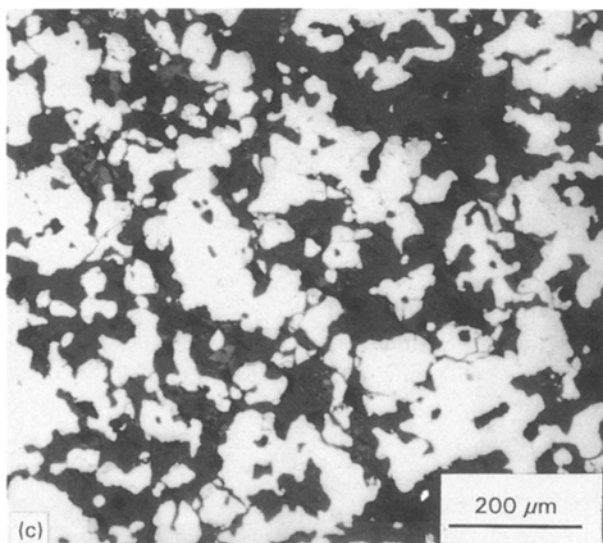
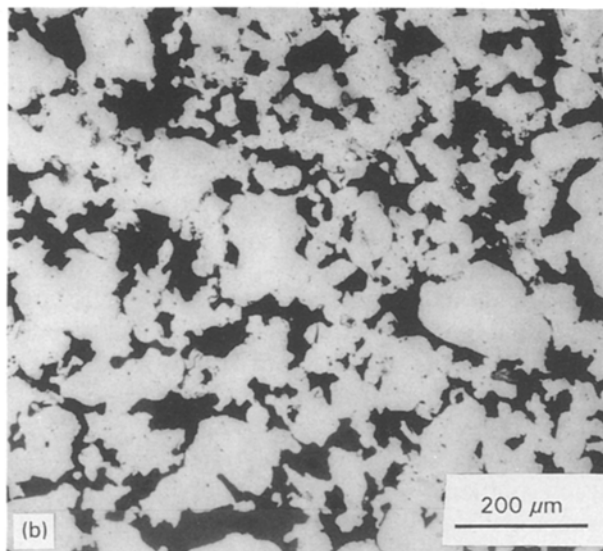
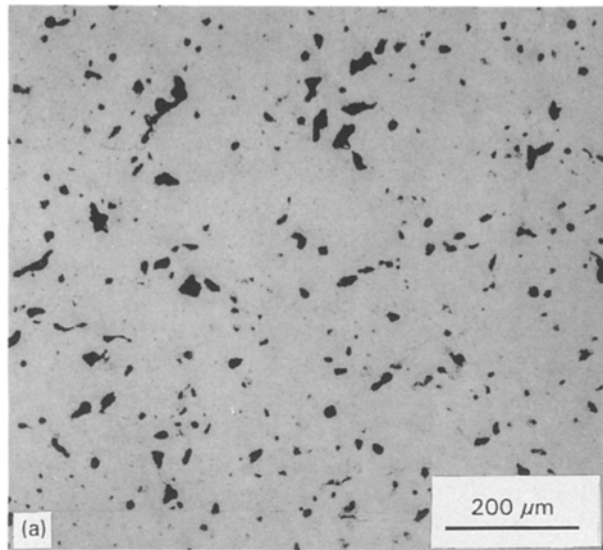


Figure 8 Porous microstructure after dilatometric measurement: (a) Ti-25Al; (b) Ti-50Al; (c) Ti-75Al (pores black).

of TiAl and Ti<sub>3</sub>Al. The thermal effects are spread over a large temperature range, thus they cannot be resolved by calorimetry. In addition, an endothermal effect owing to the transformation of α-Ti to β-Ti is visible at about 900 °C in the case of the Ti-rich Ti-25Al (Fig. 3a).

Fig. 7 shows the dimensional changes measured by dilatometer in the extrusion direction. It can be clearly recognized that swelling of specimens takes place during heating. For a given composition, the swelling becomes pronounced with increasing heating rate (Fig. 7a). At the same heating rate of 5 K min<sup>-1</sup>, the swelling increases with increasing Al content (Fig. 7b). A sudden increase of specimen length is visible at about 660 °C, the Al melting temperature, for Ti-50Al at 50 K min<sup>-1</sup> (Fig. 7a) and for Ti-75Al at 5 K min<sup>-1</sup> (Fig. 7b). This means that the specimen swelling caused by the flowing away of Al melt increases with an increasing amount of Al melt. In addition, there is a sintering effect at temperatures higher than 1000 °C; here specimen shrinkage takes place due to classical sintering mechanisms.

After cooling, the three specimens in Fig. 7b were metallographically investigated. As seen in Fig. 8, all specimens became porous. The porosity increases with increasing Al content, being in agreement with the length change measured by dilatometry (Fig. 7b).

From the results shown above it can be concluded that in order to reduce porosity, the amount of Al melt formed at the Al melting point should be decreased. This can be realized by applying a low heating rate. However this possibility is limited from a viewpoint of economy. Other possibilities are using first a low and later a high heating rate, or adding an isothermal step below the Al melting point. Both measures have already been shown to be effective [8-10].

### 3.3. HIP treatment

As shown in Figs 7 and 8, a specimen length increase of more than 20% can take place during the reaction treatment. Therefore the HIP technique is necessary

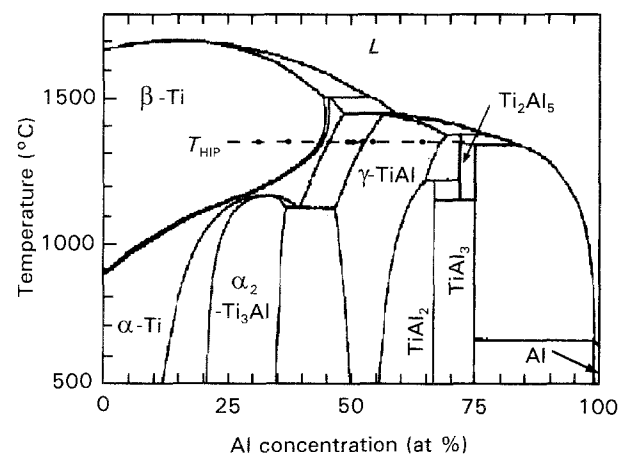


Figure 9 Phase diagram [11] with marks showing the seven alloys HIPed at 1350 °C for 5 h at 110 MPA.

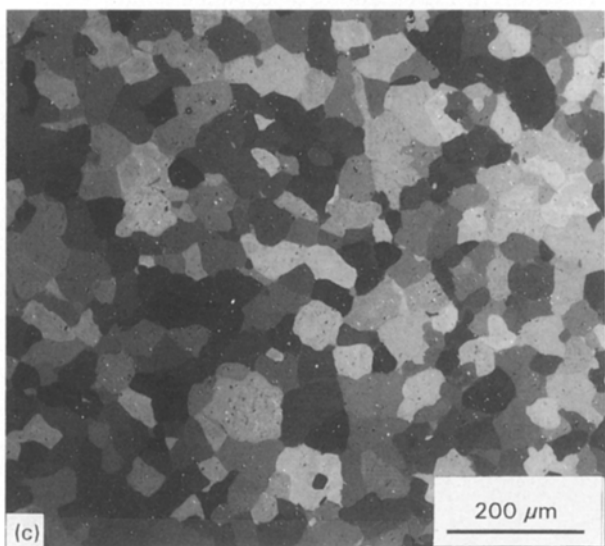
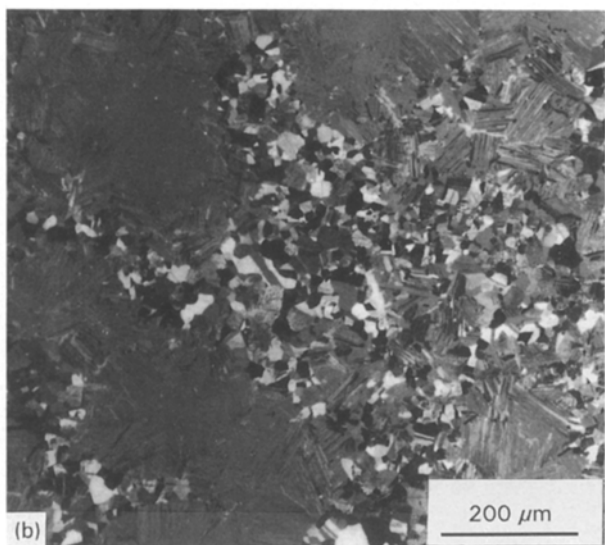
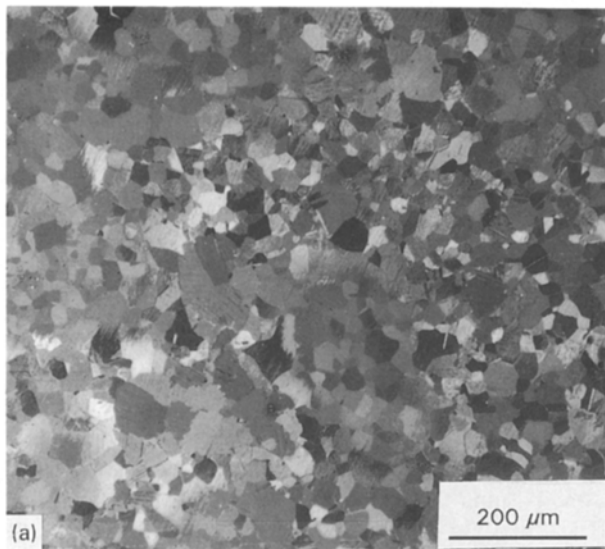


Figure 10 Microstructures of some specimens after HIP treatment at 1350 °C for 5 h at 110 MPa, as observed with polarized light in directions perpendicular to the extrusion direction: (a) Ti-31Al; (b) Ti-50Al; (c) Ti-64Al.

to compress pores. In this study, specimens of seven alloys with 10 mm diameter and 80 mm length were canned in titanium tubes by electron-beam welding and then HIPed for 5 h at 1350 °C under a pressure of 110 MPa. At the HIP temperature of 1350 °C, these alloys are located in different phase regions according to their compositions, as shown in Fig. 9. The HIPed specimens were further heat-treated at 1000 °C for 100 h in order to achieve homogeneity.

Depending on the phase regions where the HIP treatment was conducted, the alloys shown in Fig. 9 exhibit three different types of microstructure. The alloys, HIPed in the  $\beta$ -phase region, show a homogeneous microstructure with equiaxial grains (Fig. 10a). The alloys HIPed near the  $\alpha$ -transus boundary (Ti-49Al, Ti-50Al, Ti-52Al and Ti-54Al) show a partially lamellar structure, with the lamellar region appearing between the fine-grained  $\gamma$ -TiAl and the  $\alpha_2$ -Ti<sub>3</sub>Al regions (Fig. 10b). Further beyond the  $\alpha$ -transus boundary, the alloy Ti-64Al again exhibits a homogeneous equiaxial microstructure without lamellae (Fig. 10c).

#### 4. Conclusions

Titanium aluminide alloys with compositions ranging from 25 to 75 at % Al have been prepared by reaction treatment of cold-extruded elemental powder mixtures. During reaction treatment, the intermetallic phases Ti<sub>3</sub>Al, TiAl and TiAl<sub>3</sub> are formed by interdiffusion of Ti and Al. However, pore formation as an accompanying phenomenon also takes place because of the different diffusivities of Ti and Al. The processes of phase formation and pore formation were studied by means of calorimetric, dilatometric and metallographic methods. In order to reduce porosity, the amount of Al melt formed at the Al melting point should be decreased. This can be realized by applying a low heating rate, but more reasonably by using first a low and later a high heating rate, or by adding an isothermal step below the Al melting point. By applying the HIP technique, nearly fully dense specimens have been prepared. Alloys HIPed at 1350 °C for 5 h at 110 MPa show microstructures which are strongly dependent on the phase regions where the HIP treatment was conducted: a homogeneous microstructure with equiaxial grains for HIP in the  $\beta$ -phase region or further beyond the  $\alpha$ -transus boundary, and a partially lamellar structure for HIP near the  $\alpha$ -transus boundary.

#### Acknowledgements

The authors would like to thank Ms C. Peschka, Ms W.-V. Schmitz and Mr K. Wulf for technical support.

#### References

1. G. SAUTHOFF, *Z. Metallkde. Bd.* **77** (1986) 654.
2. M. DAHMS *et al.*, *ISIJ Int.* **31** (1991) 1093.
3. G.-X. WANG and M. DAHMS, *Scripta Met. Mater.* **26** (1992) 717.

4. G.-X. WANG and M. DAHMS, *Scripta Met. Mater.* **26** (1992) 1469.
5. F. J. J. van LOO and G. D. RIECK, *Acta Met.* **21** (1973) 61.
6. G.-X. WANG and M. DAHMS, *Met. Trans. A* **24A** (1993) 1517.
7. H. E. KISSINGER, *Anal. Chemie* **29** (1957) 1702.
8. G. LEITNER *et al.*, in Proceedings of International Conference on PM Aerospace Materials, 1991, (MPR Publishing, Shrewsbury, UK, 1992), p. 18/1.
9. M. DAHMS, *Z. Metallkde* (in press).
10. G. LEITNER, M. DAHMS and S. SCHULTRICH, in Proceedings of 8th International Conference on Powder Metallurgy, Vol. 2, edited by A. Salak and M. Selecka, Czechoslovakia, 1992 p. 243.
11. M. OEHRING, *J. Mater. Res.* **8** (1993) 2819.

*Received 16 February  
and accepted 8 October 1993*